Structural Engineering and Mechanics, Vol. 5, No. 6 (1997) 785-801
DOI: http://dx.doi.org/10.12989/sem.1997.5.6.785

The role of softening in the numerical analysis of R.C. framed structures

Franco Bontempi†

Department of Structural Engineering, Polytechnic of Milan, Milan, Italy

Pier Giorgio Malerba‡

Department of Civil Engineering, University of Udine, Udine, Italy

Abstract. Reinforced Concrete beams with tension and compression softening material constitutive laws are studied. Energy-based and non-local regularisation techniques are presented and applied to a R.C. element. The element characteristics (sectional tangent stiffness matrix, element tangent stiffness matrix, restoring forces) are directly derived from their symbolic expressions through numerical integration. In this way the same spatial grid allows us to obtain a non-local strain estimate and also to sample the contributions to the element stiffness matrix. Three examples show the spurious behaviors due to the strain localization and the stabilization effects given by the regularisation techniques, both in the case of tension and compression softening. The possibility to overestimate the ultimate load level when the non-local strain measure is applied to a non softening material is shown.

Key words: reinforced concrete structures; softening; localization; continuation methods.

1. Introduction

Concrete is a material which shows, both in tension and compression, a marked softening behavior. When this phenomenon is disregarded (Fig. 1a), the structural analysis gives way to behaviors which fall into the boundaries defined by the limit analysis (Bontempi, *et al.* 1995). When the softening is considered, new characteristic mechanical aspects and more detailed information about the overall structural response can be gathered (Bazant, *et al.* 1987, Ghosh and Cohn 1972, Kim and Lee 1992).

Usually the R.C. members are designed to have a ductile behavior and failure is due to the yielding of the steel, before the concrete reaches its maximum capacity. As a consequence, a particular relevance is given to the softening in the tensile states. In fact it controls the transition modes from the uncracked to the cracked state (Crisfield 1982). In a cracked R.C. element the tensile stress at a crack is zero in the concrete and is maximum in the reinforcement. Between the cracks, the tensile stresses are transferred from the steel to the concrete by the bond action which develops along the bars. The concrete, in this way, contributes in carrying the tensile forces and in increasing the overall stiffness of the structure. Several models dealing with Tension

† Assistant professor
‡ Professor

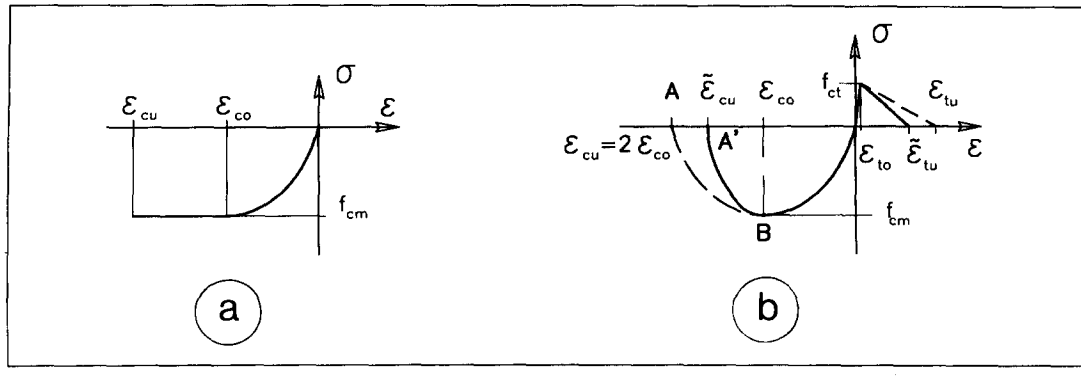

Compression (H): $\sigma=f_{CM}\frac{\varepsilon}{\varepsilon_{C0}}\left(2-\frac{\varepsilon}{\varepsilon_{C0}}\right)$	(for $\varepsilon_{C0}\le\varepsilon\le 0$): f_{CM} max compression strength corresponding to ε_{C0}
Compression (S): $\sigma=f_{CM}\frac{\varepsilon}{\varepsilon_{C0}}\left(2-\frac{\varepsilon}{\varepsilon_{C0}}\right)$	(for $\varepsilon_{CU}=2\varepsilon_{C0}\le\varepsilon\le\varepsilon_{C0}$) $E_C(\varepsilon)=\frac{d\sigma}{d\varepsilon}=\frac{2f_{CM}}{\varepsilon_{C0}}\left(1-\frac{\varepsilon}{\varepsilon_{C0}}\right)$
Tension (H): $\sigma=f_{CT}\frac{\varepsilon}{\varepsilon_{T0}}$	(for $0\le\varepsilon\le\varepsilon_{T0}$); $f_{TM}=f_{CM}/n$ max tension strength ($n=8$)
Tension (S): $\sigma=f_{CT}\left(1-\frac{\varepsilon-\varepsilon_{T0}}{\varepsilon_{TU}-\varepsilon_{T0}}\right)$	($\varepsilon_{T0}\le\varepsilon\le\varepsilon_{TU}$); $\varepsilon_{T0}=f_{TM}/E_C(0)$, $\alpha_1=\alpha+1$, $\alpha=7$, $\varepsilon_{TU}=\alpha_1\cdot\varepsilon_{T0}$

Fig. 1 Concrete constitutive laws. (a) Standard parabola rectangle stress strain relationship. (b) (Tensile softening)/(compression softening) stress-strain relationship.

Stiffening (T.S.) have been proposed (Gilbert and Warner 1978, Feenstra and de Borst 1993). Many of these models consider the contribution of the concrete in tension which surrounds the bars, by grading the length of the concrete softening branch, as shown in Fig. 1b.

However, Finite Element analysis of structures, made of strain-softening materials, may fall into unstable computations and, with mesh refining, may converge to physically inconsistent results (de Borst, *et al.* 1994). The solution may depend on the size, shape and orientation of the mesh and the model gives rise to a non-objective representation of the structural problem. As has been noted (de Borst, *et al.* 1994), these effects arise from modeling the continuum as a standard, rate independent media.

The standard stress-strain relationships are deduced from the force-displacement curves obtained from testing devices, simply by dividing the forces by the original load-carrying area and by dividing the changes in length, by the original length of the specimen. No consequences arise in the hardening phases (*H*) from this idealization; while, on the contrary, when tension and/or compression softening branches (*S*) are present, a similar criteria doesn't take the microstructure changes, which occur during the fracturing process, into account (Ottosen 1986, Planas, *et al.* 1993).

To remedy such improper structural responses due to the use of the standard continuum model, several regularisation techniques have been introduced.

2. Regularisation techniques

The regularisation techniques can be substantially derived from two basic criteria:
(1) the affine transformation of the material constitutive law, deduced by energy constraints;
(2) the non-local measure of the deformations.

2.1. Energy based affine transformation of the standard material constitutive law

We consider a unit area fiber of a holonomic material. Let H be the nominal length and $u=\varepsilon\cdot H$ the measured displacement of the reference specimen. Similarly, let $L\geq H$ and $\tilde{u}=\tilde{\varepsilon}\cdot L$ the corresponding quantities, referred to a fiber of the actual structure. In the precritical (H) tension and compression branches, the energy constraint

$$\int_0^{\tilde{u}_0}\sigma\cdot d\tilde{u}=\frac{L}{H}\cdot\int_0^{u_0}\sigma\cdot du \tag{1}$$

is, in any case, satisfied, irrespective of the fiber length, so that we can assume these curves as the effective stress-strain material laws.

In the postcritical (S) branches we impose the condition that, independently of the fiber length L, the actual fiber in tension, as well as the actual fiber in compression, absorb respectively the tension and compression energies, represented by the area below the corresponding softening curves of the reference specimen of length H_T and H_C:

$$G_C=H_C\cdot g_C=\int_{\varepsilon_{CU}}^{\varepsilon_{C0}}\sigma\cdot d\varepsilon=G_C \qquad (\forall L) \tag{2}$$

$$G_T=H_T\cdot g_T=\int_{\varepsilon_{T0}}^{\varepsilon_{TU}}\sigma\cdot d\varepsilon=G_T \qquad (\forall L) \tag{3}$$

The algebraic development of these constraints, gives rise to affine transformations of the standard constitutive laws (see Fig. 2). As shown in Fig. 1b the original tension softening branch BA, spanning from the peak strain ε_o to the ultimate strain ε_{TU}, becomes the branch B'A', spanning from the same peak strain ε_{T0}, to the adjusted ultimate strain $\tilde{\varepsilon}_{TU}=\varepsilon_{T0}\cdot(L-H_T)/L+\varepsilon_{TU}\cdot H_T/L$. An analogous transformation holds for the softening branch in compression, which ends at the adjusted ultimate strain $\tilde{\varepsilon}_{CTU}=\varepsilon_{C0}\cdot(L-H_C)/L+\varepsilon_{CU}\cdot H_C/L$. The lengths H_T, H_C are, in truth, material parameters. In F.E. meshes of framed structures, an estimate which yields to objective analysis assumes these lengths as nearly equal to the height of the beam element (Bazant, *et al.* 1987): this rule ($L\geq H_c=H_T=H$) will be respected in the following.

2.2. Non-local R.C. beam element formulation

The R.C. beam element presented by the Authors (Malerba and Bontempi 1990, Bontempi, *et al.* 1994) is improved by a non-local deformation estimate. With reference to the usual Bernoulli-Navier beam element of Fig. 3a, let $\underline{q}=[u_i\ v_i\ \varphi_i\ u_j\ v_j\ \varphi_j]$ the vector of nodal displacements, $\underline{Q}$ the vector of forces which works for $\underline{q}$, $\underline{\varepsilon}(x)$ the vector of the generalized deformations (axial strain ε_0 and curvature χ at the section x), and $\varepsilon(x,y)$ the corresponding elongation of the fiber at distance y from the beam axis.

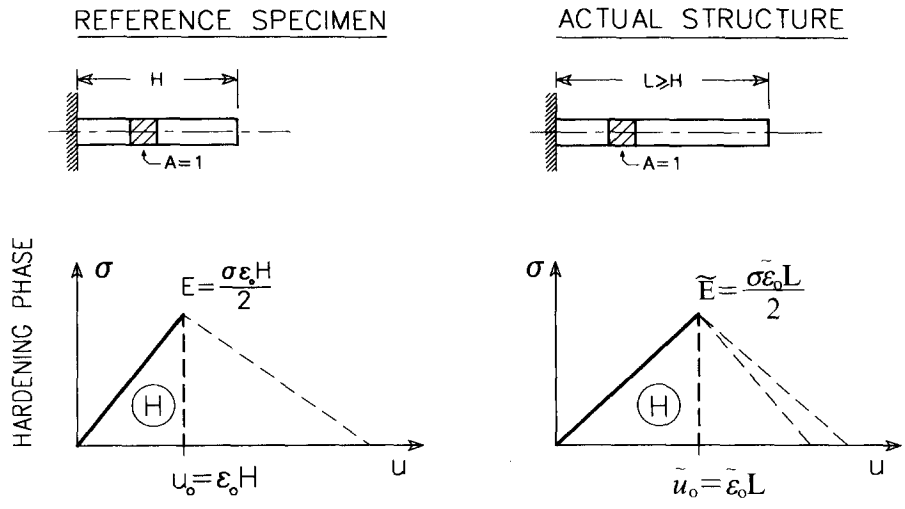

In the hardening phase (H), the energy densities of the reference specimen and of the real structure are the same:

$$E=\frac{\sigma\cdot\varepsilon_0}{2}H \qquad \tilde{E}=\frac{\sigma\cdot\tilde{\varepsilon}_0}{2}L$$

$$\frac{\tilde{E}}{L}=\frac{E}{H}\Rightarrow\tilde{E}=\frac{L}{H}E\Rightarrow\frac{\sigma\cdot\tilde{\varepsilon}_0}{2}L=\frac{L}{H}\frac{\sigma\cdot\varepsilon_0}{2}H\Rightarrow\tilde{\varepsilon}_0=\varepsilon$$

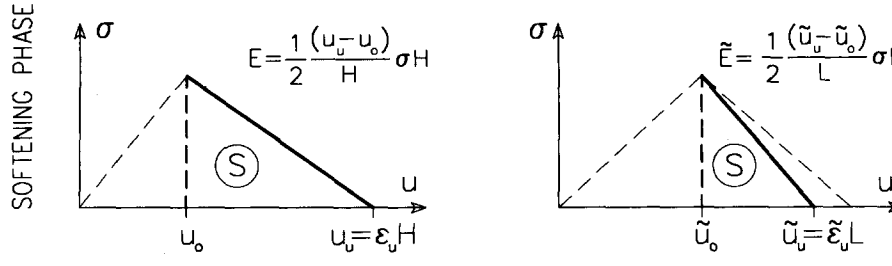

In the softening phase (S), we impose that the total energies of the reference specimen and of the real structure are the same:

$$E=\frac{1}{2}\frac{(u_u-u_o)}{H}\cdot\sigma\cdot H \qquad \tilde{E}=\frac{1}{2}\frac{(\tilde{u}_u-\tilde{u}_o)}{L}\cdot\sigma\cdot L$$

$$\tilde{E}=E\ \forall L\Rightarrow(\tilde{u}_u-\tilde{u}_o)=(u_u-u_o)\Rightarrow(\tilde{\varepsilon}_uL-\tilde{\varepsilon}_oL)=(\varepsilon_uH-\varepsilon_oH)$$

from which the following equivalent $\tilde{\varepsilon}_u$ is derived:

$$\tilde{\varepsilon}_u=\varepsilon_o\cdot(1-H/L)+\varepsilon_u\cdot(H/L)$$

Note that for $L\to H\Rightarrow\tilde{\varepsilon}_u\to\varepsilon_u$ and for $L\to\infty\Rightarrow\tilde{\varepsilon}_u\to\varepsilon_o$

Fig. 2 Derivation of the energy-based regularisation technique.

At the section of abscissa (x) the axial and transversal displacements (u_0, v_0) and the generalized strains (ε_0, χ) depend on the nodal displacements by means of the following equations:

$$\underline{u}(x)=\begin{bmatrix}u_0(x)\\v_0(x)\end{bmatrix}=\begin{bmatrix}N_1&0&0&N_4&0&0\\0&N_2&N_3&0&N_5&N_6\end{bmatrix}\cdot\underline{q}=\underline{\underline{N}}(x)\cdot\underline{q} \tag{4}$$

$$\underline{\varepsilon}(x)=\begin{bmatrix}\varepsilon_0(x)\\ \chi_0(x)\end{bmatrix}=\begin{bmatrix}N_1' & 0 & 0 & N_4' & 0 & 0\\ 0 & N_2'' & N_3'' & 0 & N_5'' & N_6''\end{bmatrix}\cdot\underline{q}=\underline{\underline{B}}(x)\cdot\underline{q} \tag{5}$$

where

$$N_1=(1-x/l);\quad N_2=[1-3\cdot(x/l)^2+2\cdot(x/l)^3];\quad N_3=l\cdot[(x/l)-2\cdot(x/l)^2+(x/l)^3] \tag{6}$$
$$N_4=(x/l);\quad N_5=[3\cdot(x/l)^2-2\cdot(x/l)^3];\quad N_6=l\cdot[-(x/l)^2+(x/l)^3]$$

In a fiber at coordinate y, of the same section, the strain in x-direction can be expressed as:

$$\varepsilon(x,y)=[1-y]\cdot\underline{\underline{B}}(x)\cdot\underline{q}=\underline{\underline{L}}(y)\cdot\underline{\underline{B}}(x)\cdot\underline{q} \tag{7}$$

and the corresponding virtual variation results:

$$\delta\varepsilon(x,y)=\underline{\underline{L}}(y)\cdot\underline{\underline{B}}(x)\cdot\delta\underline{q} \tag{8}$$

For an incremental displacement step $\Delta\underline{q}$ the strain and the stress increments are respectively:

$$\Delta\varepsilon(x,y)=\underline{\underline{L}}(y)\cdot\underline{\underline{B}}(x)\cdot\Delta\underline{q} \tag{9}$$

$$\Delta\sigma(x,y)=E_T(\varepsilon)\cdot\Delta\varepsilon(x,y)=E_T(\varepsilon)\cdot\underline{\underline{L}}(y)\cdot\underline{\underline{B}}(x)\cdot\Delta\underline{q} \tag{10}$$

and the Principle of Virtual Work states that:

$$\delta L_i=\int_0^l\int_A\delta\varepsilon\cdot(\sigma+\Delta\sigma)\cdot dA\,dx=\delta L_e=\delta\underline{q}^T\cdot\underline{Q} \tag{11}$$

The internal work can be developed as follows:

$$\delta L_i=\delta\underline{q}^T\int_0^l\underline{\underline{B}}^T(x)\cdot\int_A\begin{bmatrix}1\\ -y\end{bmatrix}\cdot(\sigma+\Delta\sigma)\cdot dA\cdot dx= \tag{12}$$

$$=\delta\underline{q}^T\left\{\int_0^l\underline{\underline{B}}^T(x)\cdot\begin{bmatrix}\int_A\sigma dA\\ -\int_A y\sigma dA\end{bmatrix}dx\right\}+\delta\underline{q}^T\left\{\int_0^l\underline{\underline{B}}^T(x)\cdot\left[\int_A\begin{bmatrix}1\\ -y\end{bmatrix}E_T\,[1-y]dA\right]\cdot\underline{\underline{B}}(x)\,dx\right\}\cdot\Delta\underline{q}=$$

$$=\delta\underline{q}^T\left\{\int_0^l\underline{\underline{B}}^T(x)\cdot\begin{bmatrix}N(x)\\ M(x)\end{bmatrix}dx\right\}+\delta\underline{q}^T\left\{\int_0^l\underline{\underline{B}}^T(x)\cdot\begin{bmatrix}\int_A E_T dA & -\int_A yE_T dA\\ -\int_A yE_T dA & \int_A y^2E_T dA\end{bmatrix}\cdot\underline{\underline{B}}(x)\,dx\right\}\cdot\Delta\underline{q}=$$

$$=\delta\underline{q}^T\left[\int_0^l\underline{\underline{B}}^T(x)\cdot\underline{r}(x)\,dx\right]+\delta\underline{q}^T\left[\int_0^l\underline{\underline{B}}^T(x)\cdot\underline{\underline{H}}(x)\cdot\underline{\underline{B}}(x)\,dx\right]\cdot\Delta\underline{q}=\delta\underline{q}^T\cdot[\underline{R}(\underline{q})+\underline{\underline{K}}_T(\underline{q})\cdot\Delta\underline{q}]$$

and lead us to define:

1) the section tangent stiffness matrix $\underline{\underline{H}}(x)$
2) the vector of the generalized stresses (the internal axial force and bending moment) $\underline{r}(x)$
3) the element tangent stiffness matrix $\underline{\underline{K}}_T(\underline{q})$
4) the element restoring force vector $\underline{R}(\underline{q})$

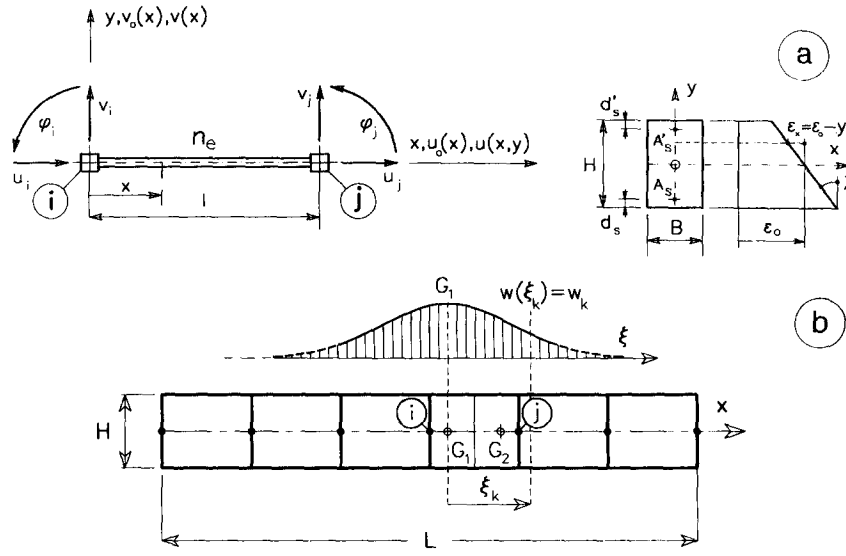

Fig. 3 a) Beam element characteristics; b) Non-local sampling technique.

Being the material non-linear, the integrals involved in such matrix operators are carried out by means of Gauss-Legendre quadratures, by adopting an adequate number of sampling sections. In dealing with the quadrature process, it must be pointed out that the sectional matrix $\underline{\underline{H}}(\underline{\varepsilon}(x))$ and the internal forces $\underline{r}(\underline{\varepsilon}(x))$ depend on the local strain vector $\underline{\varepsilon}(x)$. This dependence is sensitive to the strain localization and, with mesh refining, involves the sharp effects which lead us to the wrong aforementioned results.

To avoid the effects of this punctual, but purely conventional, sampling of the material response, a weighted strain evaluation can be introduced. With reference to Fig. 3b, let λ a characteristic length, ξ the distance between the actual Gauss point and another section of the beam, $c \in 0-1$ a tuning parameter, introduced to grade the contributions of the local and of the weighted deformations in the neighborhood of the Gauss point and $w(\xi)=\exp(-(\xi/\lambda)^2)$ a weighting function (Bazant and Chan 1984). As the non-local strain estimate, the following generalized deformations are assumed:

$$\hat{\underline{\varepsilon}} = c \cdot \underline{\varepsilon} + (1-c) \cdot \int_{-\infty}^{+\infty} \underline{\varepsilon}(\xi) \cdot w(\xi)\, d\xi \tag{13}$$

In dealing with computations λ is assumed to be equal to the beam height and the integral is computed by means of numerical quadratures in the interval $-2\lambda \leq \xi \leq +2\lambda$.

3. Solution of the equilibrium equations. —Computational aspects—

In structures made of softening materials, a local region may soften or crack, while the adjoining material unloads elastically (Crisfield 1982, de Borst 1987). The strain localization may induce dynamic jumps to a new displacement state at a fixed load level (snap-through) or dynamic jumps to a new load level under a fixed displacement state (snap-back). To catch these effects, special pseudo-static solution techniques are required.

Let $\underline{F}(t)=\lambda(t)\cdot\underline{y}$ a load vector given by the product of a scalar multiplier $\lambda(t)$ by a constant

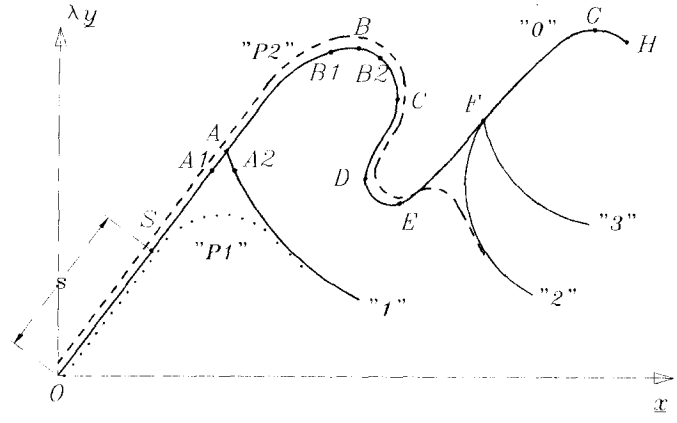

Fig. 4 Equilibrium path and its singular points.

reference force vector $\underline{y}$ and let $\underline{R}(\underline{x}(t))$ the restoring force due to the stress state corresponding to the displacement vector $\underline{x}(t)$. At the equilibrium state the vector of the residual forces

$$\underline{r}(t)=\lambda(t)\cdot\underline{y}-\underline{R}(\underline{x}(t))=\underline{0} \tag{14}$$

is zero and $\underline{x}(t)$ defines an equilibrated configuration of the structure.

The variable (t) is a fictitious time, introduced to have a reference searching parameter. By varying (t), the coordinates $\{\underline{x}(t),\ \lambda(t)\cdot\underline{y}\}$ locate a point P, which moves along the structural equilibrium path Γ shown in Fig. 4. For non-linear but elastic materials, the point P can be identified, along the path, instead of by (t), by a curvilinear abscissa (s). By differentiating Eq. (14) with respect to (s), one obtains:

$$\dot{\underline{r}}=\frac{\partial\underline{r}(s)}{\partial s}=\frac{\partial\lambda}{\partial s}\cdot\underline{y}-\frac{\partial\underline{R}(s)}{\partial\underline{x}}\frac{\partial\underline{x}}{\partial s}=\dot{\lambda}\cdot\underline{y}-\frac{\partial\underline{R}}{\partial\underline{x}}\dot{\underline{x}}=\underline{0} \tag{15}$$

in which $\partial\underline{R}/\partial\underline{x}=\underline{\underline{K}}(\underline{x}(s))$ is the symmetric tangent stiffness matrix of the structure. For small finite increments (Δs) of the abscissa (s), we can define $\Delta\underline{x}=\dot{\underline{x}}\cdot\Delta s$ and $\Delta\lambda=\dot{\lambda}\cdot\Delta s$ and state the following incremental approximation

$$\Delta\lambda\cdot\underline{y}-\underline{\underline{K}}(\underline{x}(s))\cdot\Delta\underline{x}=\underline{0} \tag{16}$$

When $\underline{\underline{K}}$ is non singular, the displacement increment $\Delta\underline{x}=\underline{\underline{K}}^{-1}\cdot\Delta\lambda\underline{y}$, corresponding to a load increment $\Delta\lambda\cdot\underline{y}$, identifies a *regular point* on the equilibrium path.

When at least one eigenvalue ω of the stiffness matrix is zero, then $det(\underline{\underline{K}})$ is zero and for a load variation $\Delta\lambda\cdot\underline{y}$ the uniqueness of the displacement increment is lost. This occurrence identifies a *singular point*, defined in more detail as follows.

Let φ the eigenvalue associated to ω. By premultiplying by φ^T the terms of Eq. (16)

$$\Delta\lambda\,\underline{\varphi}^T\cdot\underline{y}-\underline{\varphi}^T\cdot\underline{\underline{K}}\cdot\Delta\underline{x}=0 \tag{17}$$

and remembering that $\underline{\underline{K}}\cdot\underline{\varphi}=\underline{0}$ and that $\underline{\varphi}^T\cdot\underline{\underline{K}}^T=\underline{\varphi}^T\cdot\underline{\underline{K}}=\underline{0}^T$, one of these two alternatives is possible (Wagner and Wriggers 1988)

$$\underline{\varphi}^T\cdot\underline{y}=0 \text{ with } \Delta\lambda\neq0 \tag{18}$$

$$\Delta\lambda=0 \text{ with } \underline{\varphi}^T\cdot\underline{y}\neq0 \tag{19}$$

The former case represents the occurrence of a *bifurcation point* (*simple* at point A, *non-simple* at point F on the diagram of Fig. 4); the second case represents the occurrence of a *limit point* (points like B, E, G, in Fig. 4). If $\underline{\underline{K}}$ has k zero eigenvalues, a point like F is called a *non-simple bifurcation point* with multiplicity k: it has k distinct branched-off paths.

The shapes which can be assumed by the equilibrium path present other characteristic points (Fig. 4):

- in C, D the slope of Γ is infinite. However these two points can be considered all the same limit points, since by rotating the diagram around the bisecting line of the first quadrant, the tangent in C, D will once again result zero.
- H is the ultimate point defined on the basis of maximum allowable strains without material failure.

Structural imperfections or dynamic effects may shift the actual structural response from this purely ideal representation of the equilibrium state.

Let $\underline{v}$ the velocity vector corresponding to $\underline{x}$ and let $\underline{\xi}$ a generic vector of structural imperfections. From a mathematical point of view, making a reference to an ideal and perfect equilibrium path corresponds to a projection of the true one, from the actual space, where $\{\underline{x}, \underline{v}, \lambda\underline{v}, \underline{\xi}\}$ to an ideal one, where $\{\underline{x}, \underline{v}=\underline{0}, \lambda\underline{v}, \underline{\xi}=\underline{0}\}$. In this projection operation the uniqueness of the solution is lost.

When random imperfections occur, i.e., the equilibrium path is perturbed, the singular limit points tend to remain unchanged. The theory of dynamic systems calls this characteristic property *structural stability* (Troger and Steindl 1991).

With reference to Fig. 4, $P1$ and $P2$ represent two possible quasi-static perturbed paths, resembling the ideal ones identified by "1", "2", "3", but losing their bifurcation points.

In truth, when imperfections are present, the identity itself of the bifurcation points is lost. Being the real structures always affected by imperfections, only limit points in fact exist. From a theoretical point of view, the structural imperfections are accounted for so as, to assess the structural sensibility to initial conditions. In dynamics this leads us to the Theory of Chaos (Seydel 1995). In the case of R.C. structures the structural imperfections come either from non homogeneous strength or stiffness of the concrete or from dimensional non homogeneity of the structural elements and are, without any doubt, dominant aspects (Carmeliet and de Borst 1995). If on the one hand these effects lighten the computational procedures, since they tend to clear the path from the presence of bifurcation points, on the other hand they make the equilibrium paths extremely irregular, due to the softening behaviour as well as to discontinuous mechanical aspects, like cracking and section partialization.

For the solution of the non-linear problem, the Newton-Raphson (N.R.) method in its original or modified formulation, is usually adopted (Ramm 1981). The method can be considered composed of two parts: a predictor which involves the use of a load increment estimate, to make a first prediction of the $\underline{x}(t)$ next value, followed by the application of a more accurate corrector algorithm which then provides successive improvements.

Numerically, the predictor phase is the crucial one. The choice of the load increment is carried out by means of the following criteria: with reference to the tangent matrix deduced in the prediction phase, the incremental displacement vector results:

$$^{1}\Delta\underline{x} = {}^{1}\underline{\underline{K}}_{T}^{-1}({}^{1}\Delta\lambda \cdot \underline{y} + {}^{1}\underline{r}) \tag{20}$$

such an increment can be written as follows:

$$^1\Delta\underline{x} = {}^1\Delta\lambda \cdot \underline{\delta}_T + \underline{\delta}_R \tag{21}$$

where:

$$\underline{\delta}_T = {}^1K_T^{-1} \cdot {}^1\underline{y} \tag{22}$$

is the displacement vector corresponding to a linear elastic structure as having stiffness matrix K_T, and

$$\underline{\delta}_R = {}^1K_T^{-1} \cdot \underline{r} \tag{23}$$

is the displacement vector due to the residual forces.

A load variation starting from the point $\{{}^0\underline{x}, {}^0\lambda \cdot \underline{y}\}$ and moving along the equilibrium path must be defined in direction (increment or decrement) and intensity. If the load increment is too large, convergence will not occur or it will be very slow. Hence limiting criteria must be introduced.

To limit the load increment shown in Fig. 5, the tangent segment $\overline{01'}$ is scaled on the segment $\overline{01}$. Through the notation

$$^1\Delta\underline{x} = {}^1\Delta\lambda \cdot \underline{\delta}_T + \underline{\delta}_R \tag{24}$$

such a limitation can be carried out by one of these two alternatives:

- through the choice of a suitable step Δl, which extend the arc length between the already stated solution and the predicted one (*arc-length method*); such an increment can be deduced from the following quadratic equation

$$(\Delta l)^2 = {}^1\Delta\underline{x}^T \cdot {}^1\Delta\underline{x} = ({}^1\Delta\lambda \cdot \underline{\delta}_T + \underline{\delta}_R)^T \cdot ({}^1\Delta\lambda \cdot \underline{\delta}_T + \underline{\delta}_R) \tag{25}$$

which gives the opposite solutions:

$$^1\Delta\lambda = \frac{\pm \Delta l}{\sqrt{\underline{\delta}_T^T \underline{\delta}_T + \underline{y}^T \cdot \underline{y}}} \tag{26}$$

- or through a limitation on the work increment, by imposing that

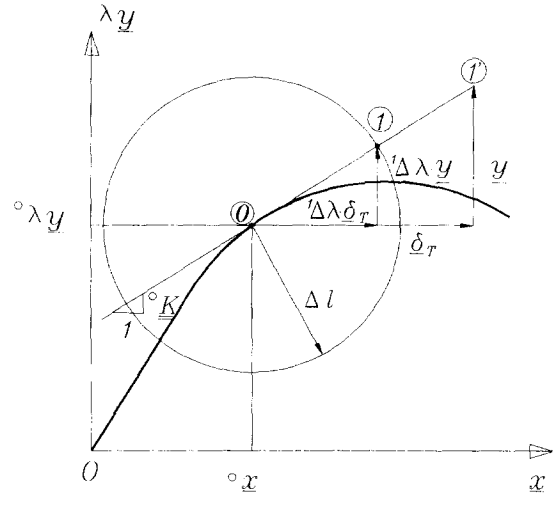

Fig. 5 Predictor phase with limitation of the load increment.

$$\Delta W=({}^{1}\Delta\lambda\cdot\underline{y}^{T})\cdot({}^{1}\Delta\lambda\cdot\underline{\delta}^{T})\leq\Delta\bar{W} \tag{27}$$

where $\Delta\bar{W}$ is a reference limiting value. The solution of the Eq. (27) gives

$${}^{1}\Delta\lambda=\pm\sqrt{\frac{\Delta\bar{W}}{\underline{y}^{T}\cdot\underline{\delta}_{T}}} \tag{28}$$

Such limitations regard not only the intensity of the load increment but also its direction, defined by one of the two signs. The choice of the sign can induce computational difficulties, i.e., loops between local loading and unloading paths. These drawbacks occur in highly irregular equilibrium paths, such as those which characterize the R.C. structures in presence of cracking and section partialisation. The use of a suitable predictor leads us to avoid the aforementioned effects. In this work, the Seydel predictor (Seydel 1984) has been used. It works through the following steps:

- The displacement increment ${}^{1}\Delta\underline{x}$, given by the previous step, is known, as well as the displacement at the beginning of the actual step:

$$\underline{\delta}_{T}={}^{1}\underline{K}_{T}\,{}^{1}\underline{y}={}^{1}\Delta\underline{x} \tag{29}$$

- Let (k) the index of the maximum absolute value of $\underline{\delta}_{T}$. The predicted increment load is

$${}^{1}\Delta\lambda=\frac{{}^{1}\Delta x_{k}}{{}^{1}\Delta x_{k}} \tag{30}$$

This load increment must be limited to 1. In other words the initial load increment, that is the load increment at the origin, can't be exceeded. Eq. (30) is in fact a local parametrization of the equilibrium path, focused on the displacement component which varies the most.

4. Examples

Both the energy based and the non-local regularization techniques have been used in a computer code dealing with the analysis of R.C. structures. Three cases are studied. They regard the structural response of the uniformly reinforced concrete beam shown in Fig. 6. In the first two cases the section of the beam is under and over-reinforced, in order to induce, respectively, softening behaviour in tension and in compression. The third case intends to show the possible effects of the non-local regularization technique, when used in the analysis of structures made of non softening materials.

4.1. Analysis of an under-reinforced concrete beam

The section of the beam is shown in Fig. 6. The aim of the example is to highlight the effects due to the following choices (1) whether to consider the concrete softening or not; (2) the different discretisations; (3) the different regularisation techniques. The mesh is progressively refined by subdividing the two spans of the structure into $(i+3i,\ i=1,\ 10)$ elements of equal length. The results are given in terms of load displacement curves $(P-q)$. In order to have a common reference behaviour, the beam is studied in advance by adopting the stress-strain parabola-rectangle law of Fig. 1a. and through the direct iteration (secant) method. The results,

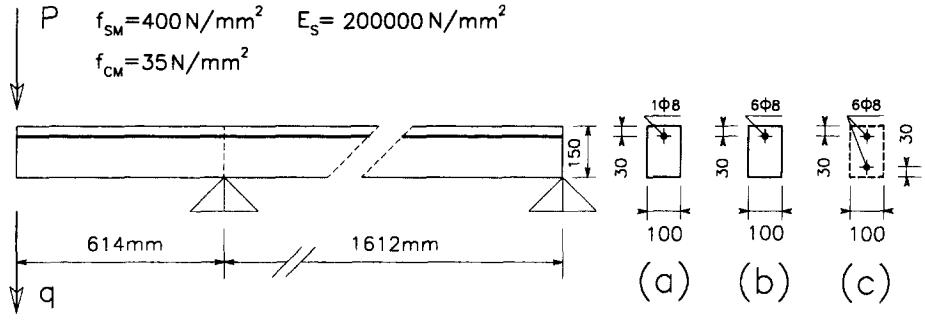

Fig. 6 Geometrical and reinforcement characteristics of the beam analyzed in the examples.

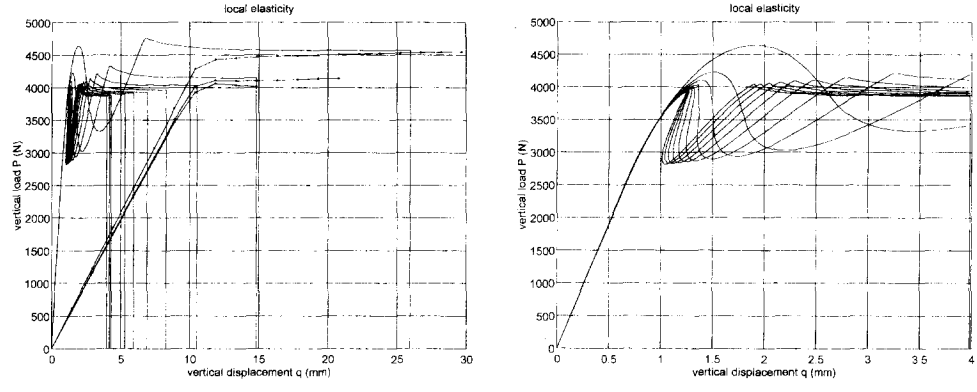

(a) (b)

Fig. 7 (a) Load displacement curves obtained through non-softening and softening material constitutive laws (Fig. 1a, b) without any regularisation technique. (b) Enlargement of the transition zone to the cracked stage.

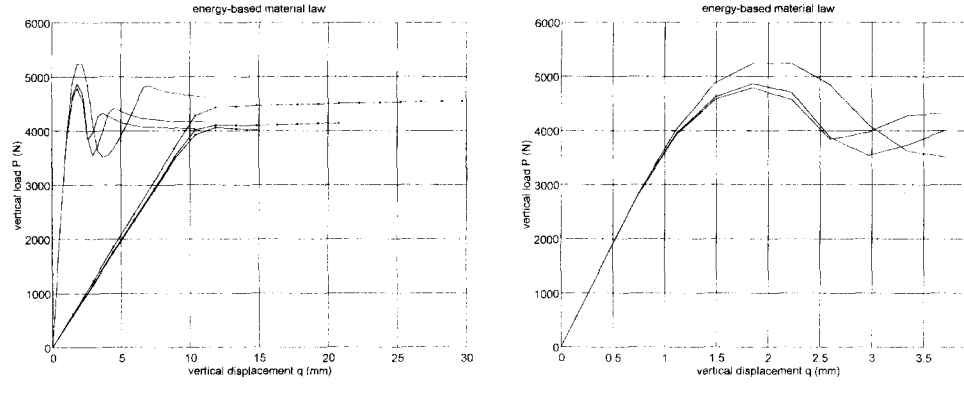

(a) (b)

Fig. 8 (a) Load displacement curves obtained through non-softening and softening material constitutive laws and the energy based regularisation. (b) Enlargement of the transition zone to the cracked stage.

obtained respectively by means of (1+3), (2+6), (4+12) elements, are represented by the curves identified by the black dots and are repeated in all the other cases which are studied.

4.1.1. Analysis without regularisation techniques

By modeling the concrete through the tension-compression softening constitutive law of Fig. 1b and by subdividing the beam of Fig. 6 into ($i+3i$, $i+1$, 10) elements, the local sampling without any regularisation technique, gives the family of curves shown in Fig. 7a, b. One observes that:

(1) the ultimate load, for all the solutions, is almost the same;
(2) the introduction of a tension resistance strongly increases the stiffness in the initial nearly elastic branch and no differences arise in this branch from the mesh refinement;
(3) the ultimate displacement values, for all the solutions, progressively decrease;
(4) in presence of softening, the transition from the first to the second branch of these curves takes place with a sharp load fall, followed by a stiffening branch which moves towards the conventional tension stiffening ascending curve, usually considered in the design;
(5) the close-up of the transition zone, shown in Fig. 7b, highlights how these solutions are strongly affected by the density of the mesh, as far as converging to non-physical snap-back effects for those more highly refined.

This mesh depending behaviour can be explained by observing the cracking patterns shown in Fig. 10a, where the dark shadowed zones contour the crack development in their depth and in their span directions, at the ultimate state: finer meshes reduce the span of the cracks and the curvature localization induces the sharp effects already shown. This is also evident from the displacement fields of Fig. 11a.

4.1.2. Analysis with energy based regularisation

Figs. 8a, b show the load displacement curves obtained for the same structure adopting the

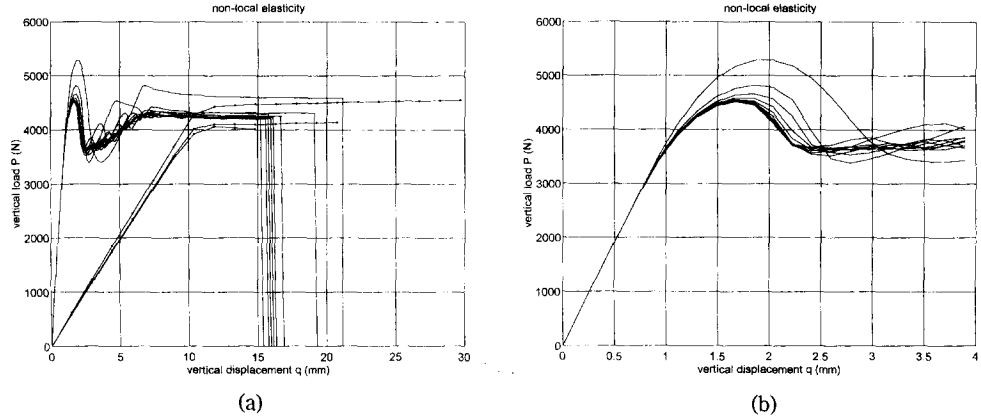

(a) (b)

Fig. 9 (a) Load displacement curves obtained through non-softening and softening material constitutive laws and the non-local regularisation technique. (b) Enlargement of the transition zone to the cracked stage.

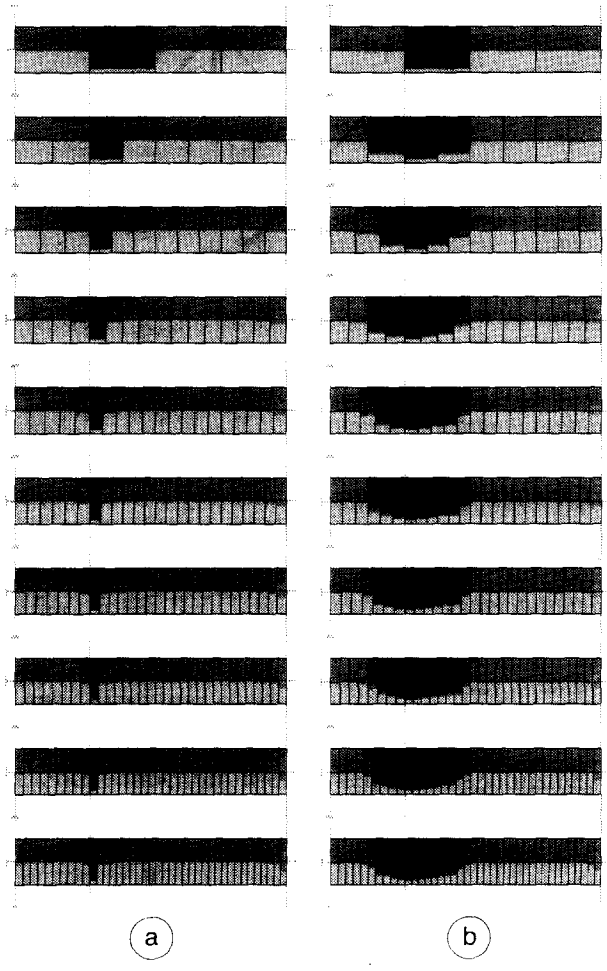

Fig. 10 Crack patterns on the surface of the beam. (a) Crack localization obtained adopting the softening constitutive law and without any regularisation technique. (b) Cracked elements diffusion according to the non-local deformation estimate.

energy adjusted material constitutive law. The snap-back effects disappear. With mesh refining the load-displacement curves corresponding to the succession of the meshes, converge on a same path and finish with the same ultimate displacement. Only the meshes (1+3), (2+6), (3+9) are studied, because of the limiting condition $H \leq l$, being l the length of the element.

4.1.3. Analysis with non-local deformation estimate

With mesh refining, the effects of this regularisation technique clearly appear from the evolution of the load-displacement curves drawn in Fig. 9a. In comparison to the results of the previous case (Fig. 8b), the details of the transition zone (Fig. 9b), show, in this case, a more orderly and faster convergence process. A physical explanation to this tendency can be deduced by the inspection of Fig. 10b, where, as a consequence of the non-local sampling of deformations, the cracks are spread over a wider area; the crack contours result more smoothly diffused on

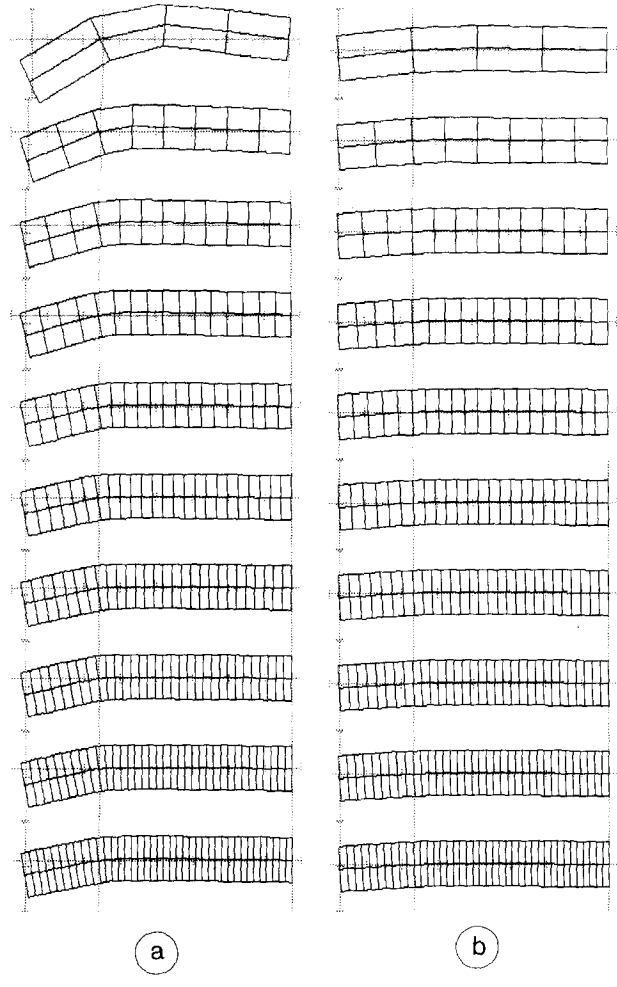

Fig. 11 Displacement fields for the beam: (a) Adopting the softening constitutive law and without any regularisation technique, (b) according to the non-local deformation estimate.

the surface of the beam and, furthermore, the envelope of the cracked zones results nearly constant for all the meshes. In Fig. 11b the corresponding displacement fields are shown.

4.2. Analysis of an over-reinforced concrete beam

The section of the beam is shown in Fig. 6b. Being the beam over-reinforced, the compression softening branch of the constitutive law will be activated. The load deflection curves, given by the same mesh succession as in the previous case, are shown in Fig. 12. Neither snap-through nor spurious snap-back effects are now present. With mesh refining, the curves converge to an asymptotic behaviour near the one corresponding to the finest mesh. The softening branch tends to exhibit an almost vertical load fall, which highlights the fragile character of the compression failure, typical of strongly reinforced beams.

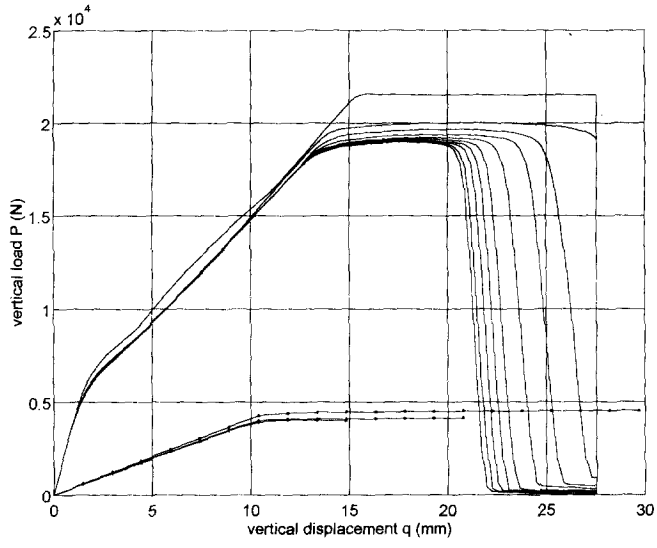

Fig. 12 Load displacement curves obtained through non-local regularisation technique for the overreinforced beam (6Φ8) having the section of Fig. 6b.

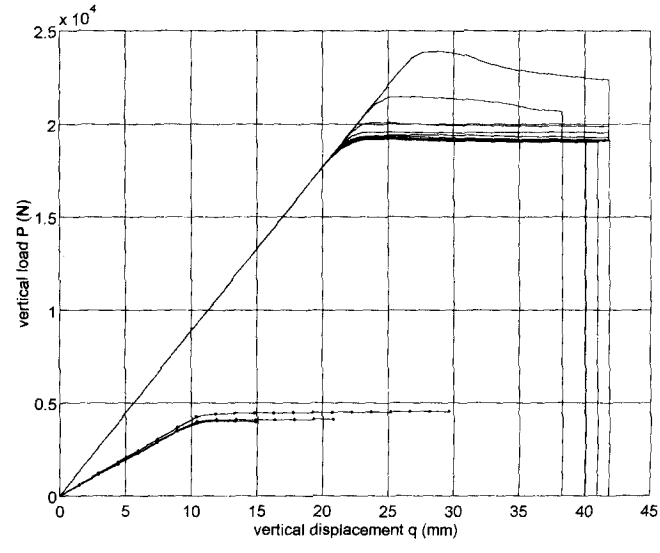

Fig. 13 Load displacement curves obtained through non-local regularisation technique for the elastic-plastic beam (6Φ8+6Φ8), having section of Fig. 6c.

4.3. Analysis of a beam having an ideal section made of non softening material

As shown in Fig. 6c, the section of the beam is composed of two bars, which work as top and bottom stringers. Such stringers are ideally connected by the internal kinematic constraint, which compels a segment, straight and normal to the axis of the beam, to remain straight and normal in the deformed shape. The load deflection curves, given by the same mesh succession as in the previous case, are shown in Fig. 13. Through simple hand calculations, the ultimate

load results $P_u = 17683$N. Even if the constitutive law assumed for the steel doesn't present softening branches, the non-local strain estimate has been adopted all the same. With mesh refining the results converge to a stable solution having $P_u = 19000$N. This value of P_u is 7.45% higher than the exact one. This is due to the smoothing effects implicit in using non-local techniques, which clearly underestimate the punctual deformation. This effect, however, can be easily corrected by adjusting the nominal value of the material strength.

5. Conclusions

A non-linear analysis of under/over-reinforced concrete beams up to collapse and allowing for strain softening effects has been presented.

In the presence of strain softening, the use of the smeared crack model and of the simple strength criterion to analyze the crack propagation, may lead to non objective results, since computational predictions may be strongly influenced by the choice of the element size.

The use of regularisation techniques permits us to avoid the spurious effects due to the strain localization. The essentials of such techniques, based (a) on the affine transformation of the material constitutive law or (b) on the non-local measure of the deformations, are recalled and applied to a R.C. beam element. The element characteristics are derived and the expressions of the sectional tangent stiffness matrix, the generalized stresses, the element tangent stiffness matrix and the restoring forces are given.

The search for the equilibrium path has been carried out by means of a tangent algorithm based on the Seydel predictor, particularly robust in dealing with highly irregular equilibrium paths.

The numerical examples present the load deflection curves up to collapse and a close-up of the transition zones from the uncracked to the cracked state. For different reinforcement amounts, the various results obtained by either adopting the regularisation techniques or not, are shown and compared. A further comparison between the crack patterns at the load which precedes the collapse, gives a physical explanation to the effects of the strain localization as well as to the stabilization action of the non-local deformation estimate. When applied to an elastic-plastic material, smoothing effects due to the non-local technique may lead to overestimating the ultimate load level but that aspect can be easily corrected.

Acknowledgements

The Authors thank the Italian Ministry of University and Research Technology for its financial support (Grant MURST 60%/93 to the Dept. of Civil Eng., Udine University). The Post Graduated School in Reinforced Concrete Structures "F.lli Pesenti" of the Polytechnic of Milan is acknowledged for the use of its computational tools.

References

Bazant, Z.P. and Ta-Peng Chan, (1984), "Instability of non-local continuum and strain averaging", *J. of Eng. Mech. ASCE*, **110**(10), 1441-1450.

Bazant, Z.P., Pan, J. and Pijaudier-Cabot, G., (1987), "Softening in reinforced concrete beams and frames", *J. of Eng. Mech. ASCE*, **113**(12), 2333-2347.

Bontempi, F., Malerba, P.G. and Romano, L., (1995), "A direct secant formulation for the reinforced and prestressed concrete frame analysis", *Studi e Ricerche*, **16**, Scuola di Specializzazione in Costruzioni in C.A., Politecnico di Milano (in Italian).

Carmeliet, J. and de Borst, R., (1995), "Stochastic approaches for damage evolution in standard and non standard continua", *Int. J. of Solids and Structures*, **32**(8/9), 1149-1160.

Crisfield, M.A., (1982), "Local instabilities in the non-linear analysis of reinforced concrete beams and slabs", *Proc. Instn. Civ. Engrs.*, Part 2, 73, 135-145.

de Borst, R., (1987), "Computation of post-bifurcation and post-failure behaviour of strain-softening solids", *Computers & Structures*, **25**(2), 211-224.

de Borst, R., Carmeliet, J., Pamin, J. and Sluys, L.J., (1994), "New horizons in computer analysis of damage and fracture in quasi-brittle solids", *Fracture and Damage in Quasibrittle Structures*, edited by Z.P. Bazant, M. Jirasek and J. Mazars, E&FN.

Feenstra, P.H. and de Borst, R., (1993), "Aspects of robust computational modeling for plain and reinforced concrete", *HERON*, **38**(4).

Ghosh, S.K. and Cohn, M.Z., (1972), "Non-linear analysis of strain softening structures", *Inelasticity and Non-Linearity in Structural Concrete*, University of Waterloo Press.

Gilbert, R.I. and Warner, R.F., (1978), "Tension stiffening in reinforced concrete slabs", *J. of Struct. Eng., ASCE*, **104**(ST12), 1885-1900.

Kim, J.K. and Lee, T.G., (1992), "Non-linear analysis of reinforced concrete beams with softening", *Computers & Structures*, **44**(3), 567-573.

Malerba, P.G. and Bontempi, F., (1990), "Material and geometrical non-linear analysis of reinforced concrete frames", *EPMESC III, Int. Conf. on Education, Practice and Promotion of Comput. Methods in Engineering using Small Computers*, Macao, August. Vol. I, 121-132.

Ottosen, N.S., (1986), "Thermodynamic consequences of strain softening in tension", *J. of Eng. Mech., ASCE*, **112**(11), 1152-1164.

Planas, J., Elices, M. and Guinea, G.V., (1993), "Cohesive cracks versus non-local models: closing the gap", *Int. J. of Fracture*, No.63, 173-187.

Ramm, E., (1981), "Strategies for tracing the non-linear response near limit points", *Non-linear Finite Element Analysis in Structural Mechanics*, W. Wunderlich, E. Stein, K.J. Bathe Editors, Springer Verlag, Berlin.

Seydel, R., (1984), "A continuation algorithm with step control", *International Series of Numerical Mathematics*, **70**, Birkhauser Verlag Basel.

Seydel, R. (1988), *From Equilibrium to Chaos: Practical bifurcation and stability analysis*, Elsevier Science Publishing Co. Inc., N.Y.

Troger, H. and Steindl, A., (1991), *Non-linear Stability and Bifurcation Theory*, Springer-Verlag, Wien.

Wagner, W. and Wriggers, P., (1988), "A simple method for the calculation of postcritical branches", *Eng. Computations*, **5**, June, 103-109.